# Self-Assembled LiFePO4/C Nano/Microspheres by Using Phytic Acid as Phosphorus Source

**ARTICLE** *in* THE JOURNAL OF PHYSICAL CHEMISTRY C · FEBRUARY 2012

Impact Factor: 4.77 · DOI: 10.1021/jp212063e



**6 AUTHORS**, INCLUDING:

Jing Su
Chinese Academy of Sciences
**18** PUBLICATIONS **474** CITATIONS
SEE PROFILE

Xing-Long Wu
Northeast Normal University
**61** PUBLICATIONS **3,168** CITATIONS
SEE PROFILE

Jong-Sook Lee
Chonnam National University
**79** PUBLICATIONS **971** CITATIONS
SEE PROFILE

Yu-Guo Guo
Chinese Academy of Sciences
**170** PUBLICATIONS **10,870** CITATIONS
SEE PROFILE

THE JOURNAL OF PHYSICAL CHEMISTRY C

Article

pubs.acs.org/JPCC

# Self-Assembled $LiFePO_4$/C Nano/Microspheres by Using Phytic Acid as Phosphorus Source

Jing Su,[†] Xing-Long Wu,[†] Chun-Peng Yang,[†] Jong-Sook Lee,[‡] Jaekook Kim,[‡] and Yu-Guo Guo*,[†]

[†]Beijing National Laboratory for Molecular Sciences (BNLMS), Institute of Chemistry, Chinese Academy of Sciences (CAS), Beijing 100190, P. R. China

[‡]School of Materials Science and Engineering, Chonnam National University (WCU), Gwangju 500-757, Republic of Korea

Supporting Information

**ABSTRACT:** A general and efficient hydrothermal strategy combined with a high-temperature carbon-coating technique has been developed for large scale synthesis of self-assembled $LiFePO_4$/C nano/microspheres employing the biomass of phytic acid as a novel and eco-friendly phosphorus source. The $LiFePO_4$/C nano/microspheres are investigated by SEM, TEM, EDS, XRD, Raman spectroscopy, and electrochemical techniques. A reasonable assembly process of the hierarchical structure is proposed on the basis of time-dependent experimental results. Because of the unique structure, the $LiFePO_4$/C nano/microspheres show a high tap density of 1.2 g $cm^{-3}$, a high reversible specific capacity of 155 mA h $g^{-1}$ at 0.1 C, as well as excellent rate capability and cycling performance, exhibiting great potential as superior cathode materials in lithium ion batteries. The approach for the preparation of $LiFePO_4$ by using PA as the phosphorus source may open new prospects for utilization of biomass to produce high performance cathode materials for lithium ion batteries.

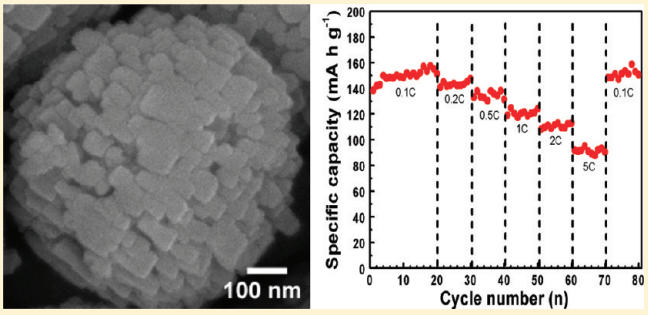


## 1. INTRODUCTION

Developing eco-friendly devices and related advanced materials is a key point to satisfy the ever-growing demands for a clean environment and sustainable energy sources. Over the last decades, rechargeable lithium ion batteries (LIBs), as salient power sources from popular portable electronics to emerging electric vehicles, have been capturing considerable attention due to their lightweight, high energy density, and long cycle life.[1−3] Recently, intensive efforts have been put into exploring alternatives to the costly and relatively unsafe cobalt−oxide-based cathodes presently dominated in commercialized LIBs. Among the proposed cathode materials, olivine-structured $LiFePO_4$ has attracted immense interest as a promising candidate due to its appealing features, such as low cost, high theoretical capacity (170 mA h $g^{-1}$), superb stability, and environmental compatibility.[4−6] Despite these advantages, $LiFePO_4$ has inherently poor electrical conductivity and sluggish lithium ion motion ability, which hinders its wide applications in powerful LIBs.[7,8] Up to now, modifications of $LiFePO_4$ by decreasing particle size through various synthesis techniques,[9−15] doping with foreign atoms,[5,6,16,17] and coating with electronically conductive agents[6,18−23] have been reported as effective ways to enhance its kinetics. In addition, it has been reported that constructing electrode materials with self-assembled nano/micro hierarchical structures is one of the most desirable structures of choice to improve the lithium storage properties because they can combine the advantages of high specific capacity and enhanced kinetics of nanometer-sized building blocks and good stability of micrometer-sized assemblies.[24−28]

In recent years, naturally biological materials, which are abundant, renewable, and eco-friendly, have been used to fabricate a wide range of inorganic materials with novel morphologies and properties.[29−33] Phytic acid (PA), with the chemical formula of $C_6H_6(H_2PO_4)_6$ known as inositol hexakisphosphate, is a common natural compound containing six carbon atoms and six phosphate groups in its molecule, as shown in Figure 1. The biomass is the principal storage form of

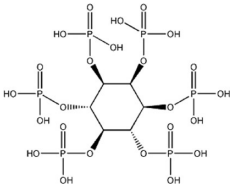

**Figure 1.** Chemical formula of phytic acid.

phosphorus in many plant tissues, and it can chelate many mineral ions such as $Zn^{2+}$, $Fe^{2+}$, $Fe^{3+}$, $Ca^{2+}$, and $Mg^{2+}$ owing to its high negative charges on the surface.[34] In view of the high phosphorus content, extensive sources and strong interaction

**Received:** December 14, 2011
**Revised:** January 31, 2012
**Published:** February 1, 2012

with $Fe^{2+}$, PA is a fresh and promising organic phosphorus source for the synthesis of $LiFePO_4$ compared with the commonly used $NH_4H_2PO_4$, which contains ammonium cations and leads to the emission of corrosive $NH_3$ gas during the synthesis process. In addition, considering the inherent symmetric structure, it is expected that PA might have a pronounced influence on the formation of novel $LiFePO_4$ structures.

Herein, we report a facile, large-scale, and low-cost hydrothermal strategy to synthesis self-assembled $LiFePO_4$ nano/microspheres by using PA as a novel and green phosphorus source. While the nanosized building blocks of $LiFePO_4$ can decrease the $Li^+$ migration length and improve the kinetics of $LiFePO_4$,[13,25] the microsized assemblies in the form of spherical structure are expected to guarantee a high tap density, which is highly desired for building high volumetric energy density LIBs.[21,23] A high electronically conductive carbon coating layer is introduced to the surface of the $LiFePO_4$ spheres by high temperature vapor deposition of $C_2H_2$ gas. The as-obtained $LiFePO_4$/C nano/microspheres do show a high tap density of 1.2 g $cm^{-3}$, a high reversible specific capacity of 155 mA h $g^{-1}$ at 0.1 C, as well as excellent rate capability and cycling performance.

## 2. EXPERIMENTAL SECTION

**2.1. Synthesis.** All chemicals used were purchased without further purification. Phytic acid (Aladdin Chemistry Co., Ltd., 50%) and $LiOH·H_2O$ (Alfa Aesar, 98%) were dissolved in distilled water to form a brownish yellow transparent solution. $FeSO_4·7H_2O$ (Sigma-Aldrich) solution was then added into the above solution under vigorous magnetic stirring. All PA and $FeSO_4$ are assumed to take part into the reaction during the hydrothermal process. The molar ratio of PA/$FeSO_4$/LiOH is 1:6:18, to realize a molar ratio of Li/Fe/P = 3:1:1 in the starting solution. After bubbling with high-pure $N_2$ for 0.5 h, the obtained solution was quickly transferred into a Teflon-lined stainless steel autoclave, heated at 180 °C for 6 h, and then cooled to room temperature naturally. The as-prepared precipitation was collected by centrifuging, repeatedly washed by distilled water and absolute alcohol, and finally dried at 60 °C in air for 8 h. Carbon-coating of the as-obtained $LiFePO_4$ material was carried out in a tube furnace heated at 675 °C for 12 h under a mixed atmosphere of Ar (95%) and $H_2$ (5%), then 50% of high-purity acetylene gas was introduced into the system at a flow rate of 30 $cm^3$ $min^{-1}$ for 0.5 h. After being taken out from the furnace at room temperature, the color of the sample was changed to black from gray.

**2.2. Structural Characterization.** X-ray powder diffraction (XRD) analyses of the as-obtained samples were carried out with a Rigaku D/max-2500 with Cu K$\alpha$ radiation ($\lambda$ = 1.54056 Å) operated at 40 kV and 200 mA. A field-emission scanning electron microscope (SEM, JEOL 6701F) and transmission electron microscope (TEM, Tecnai F30) were used to investigated the morphology and particle size of the products. The microstructure of the samples was determined using a high-resolution transmission electron microscope (HRTEM) on a JEM-2010 apparatus with an acceleration voltage of 200 kV. Raman measurements were performed using a DXR from Thermo Scientific with a laser wavelength of 532 nm. Elemental compositions of the samples were determined by an energy-dispersive X-ray spectroscopy (EDS, Phoenix) system, and the content of carbon was examined by a Leco CS-344 infrared carbon−sulfur meter. Tap density of the product was measured by a Tap denser (HY-100, Dan Dong Hylology Instrument Co., Ltd.). Powders were loaded into a cylinder and then tapped for at least 10 min with 300 taps $min^{-1}$ frequency.

**2.3. Electrochemical Characterization.** Electrochemical tests were carried out using two-electrode Swagelok-type cells assembled in an argon-filled glovebox. For preparing the working electrodes, a mixture of active material, carbon black, and poly(vinyl difluoride) with a weight ratio of 70:20:10 was pasted on Al foil. A glass fiber (GF/D) from Whatman was used as a separator, and lithium foil was used as a counter electrode. The electrolyte was 1 M $LiPF_6$ dissolved in a mixture of ethylene carbonate (EC), dimethyl carbonate (DMC), and ethyl methyl carbonate (EMC) with a volume ratio of 2:3:5 (Tianjin Jinniu Power Sources Material Co., Ltd.). Cyclic voltammetry (CV) was carried out using an Autolab PG302N at a scan rate of 0.1 mV $s^{-1}$ in the potential range of 2.2−4.2 V (vs $Li^+$/Li). Galvanostatic charge/discharge of the assembled cells was performed on an Arbin BT2000 system in the voltage range of 2.2−4.2 V (vs $Li^+$/Li). The C-rate used was based on the theoretical capacity of $LiFePO_4$ (170 mA h $g^{-1}$). All electrochemical measurements were carried out at room temperature.

## 3. RESULTS AND DISCUSSION

**3.1. Structural Analysis and Morphology Characterization.** The XRD patterns of the as-synthesized $LiFePO_4$ before and after carbon coating are shown in Figure 2. All

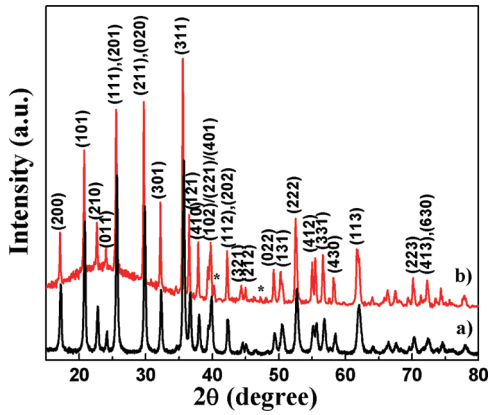


**Figure 2.** XRD patterns of the as-synthesized $LiFePO_4$ products (a) before and (b) after carbon-coating. Peaks denoted with an asterisk (*) belong to $Fe_2P$.

reflections of the $LiFePO_4$ sample achieved by the hydrothermal reaction at 180 °C (Figure 2a) can be well indexed to pure $LiFePO_4$ with an orthorhombic olivine-type structure (JCPDS card No. 40−1499). The strong diffraction peaks in the pattern indicate the highly crystalline nature of the $LiFePO_4$ sample. After subsequent heat treatment and carbon coating (Figure 2b), the resulted $LiFePO_4$/C composite still remains in the crystalline $LiFePO_4$ phase. An additional broad diffraction peak at 20−30° corresponding to carbon appears in the XRD pattern, which indicates the nonwell crystalline nature of the carbon coating.[35] In addition, $Fe_2P$ is visible in the diffraction pattern, which generally forms by the reduction of Fe and P ions in the presence of hydrogen and acetylene, and was reported favorable for improved electrochemical performance due to its good electrical conductivity.[6,36,37] The existence of carbon in the samples was further confirmed by a Raman


dx.doi.org/10.1021/jp212063e | J. Phys. Chem. C 2012, 116, 5019−5024

spectrum, as shown in Figure S1 in the Supporting Information. The peaks at 900−1120 $cm^{-1}$ could be assigned to the $PO_4^{3-}$ characteristic intramolecular stretching modes in $LiFePO_4$ lattice,[38] while two broad bands in the range of 1170−1460 $cm^{-1}$ and 1470−1730 $cm^{-1}$ are attributed to the disordered graphite and crystalline graphite, respectively. These results prove the successful preparation of carbon coated $LiFePO_4$ products.

Figure 3a displays a typical SEM image of the as-synthesized $LiFePO_4$ products. It can be clearly observed that the sample is

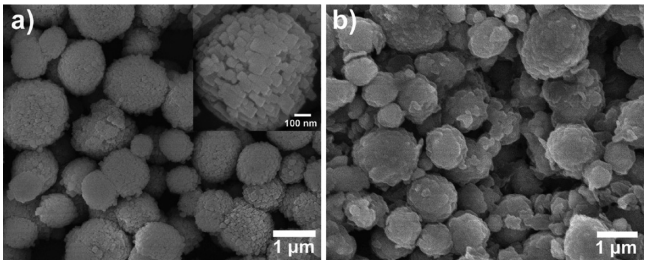


**Figure 3.** SEM images of the as-synthesized $LiFePO_4$ nano/microspheres (a) before and (b) after carbon coating.

mainly composed of microspheres with diameter from 0.5 to 2 μm. The inset in Figure 3a shows a high-magnification SEM image of a single $LiFePO_4$ microsphere, which is made from many nanoparticles. These tiny building blocks are assembled side by side in an ordered fashion. After calcination and carbon-coating, the resulted $LiFePO_4$/C composite still retains the same morphology and structure as the $LiFePO_4$ hierarchical nano/microspheres (Figure 3b). The success preparation of $LiFePO_4$ and $LiFePO_4$/C were further confirmed by the elemental signatures of Fe, P, O, and C in their EDS patterns (Figure S2 in Supporting Information). The existence of trace carbon in the $LiFePO_4$ sample synthesized by the only hydrothermal route (Figure S2a in Supporting Information) could be attributed to the carbon rings in the PA molecules. After carbon coating, the elemental maps demonstrate that the $LiFePO_4$ microspheres are evenly coated by carbon, and the elemental analysis indicates that the amount of carbon in the composite is about 15 wt % (Figure S2b in Supporting Information). The measured tap density of the $LiFePO_4$/C nano/microspheres is as high as 1.2 g $cm^{-3}$, which is much higher than that of pristine $LiFePO_4$/C nanoparticles (ca. 0.6−1.0 g $cm^{-3}$). The high tap density is of great importance for the transportation application of LIBs because it promises high volumetric energy densities.[23]

To better understand the morphology and microstructure of the $LiFePO_4$ nano/microspheres before and after carbon coating, TEM and HRTEM observations were performed. The typical TEM image shown in Figure 4a further confirms that the as-obtained $LiFePO_4$ sample consists of microspheres assembled from tiny nanoparticles, which is in good agreement with the above SEM observations. It is worth mentioning that the nano/microspheres are robust structures that they cannot be destroyed into fragments or dispersed nanoparticles even under ultrasonic treatment. The HRTEM image taken from the edge of a $LiFePO_4$ nano/microsphere displays clear crystal lattices with *d*-spacing of 0.29 nm, corresponding to (020) planes of orthorhombic phase $LiFePO_4$ (Figure 4b). The TEM image of $LiFePO_4$/C microspheres (Figure 4c) shows that the microspheres are wrapped by a thin film of carbon with

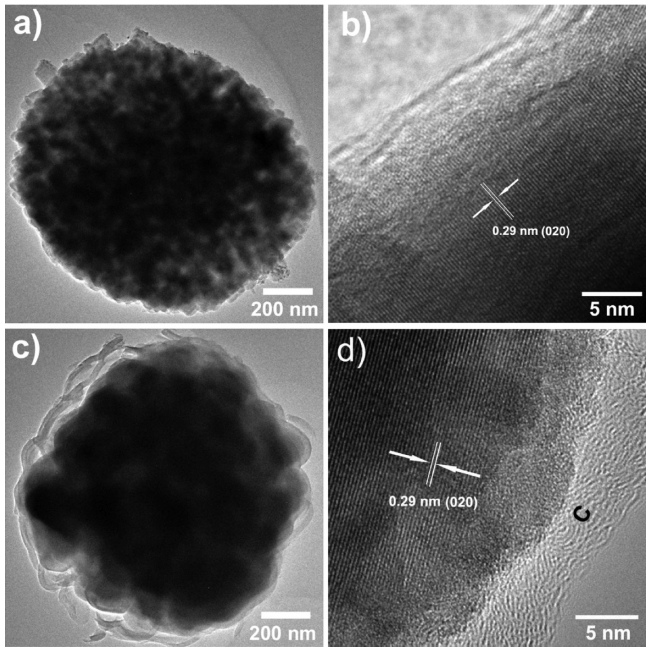


**Figure 4.** TEM images of the as-synthesized $LiFePO_4$ nano/microspheres (a,b) before and (c,d) after carbon-coating.

nanometer-sized voids between the particles and the carbon nanocoating layers. The feature promises the formation of a large number of active triple-phase (i.e., C, $LiFePO_4$, and liquid electrolyte) contacts in the system, which are favorable for fast Li insertion/extraction when the materials are used as cathode materials in LIBs.[18,23] In addition, it can also be seen from the HRTEM image that an amorphous carbon coating layer with a thickness of 4−6 nm uniformly covered on the surface of $LiFePO_4$ grains (Figure 4d), which is in good agreement with the above XRD result (see Figure 2b).

**3.2. Formation Mechanism.** In order to gain insight into the formation mechanism of the $LiFePO_4$ nano/microspheres, time-dependent experiments were carefully carried out. First, the samples prepared at regular reaction time intervals were investigated by XRD. As shown in Figure 5a, the XRD pattern

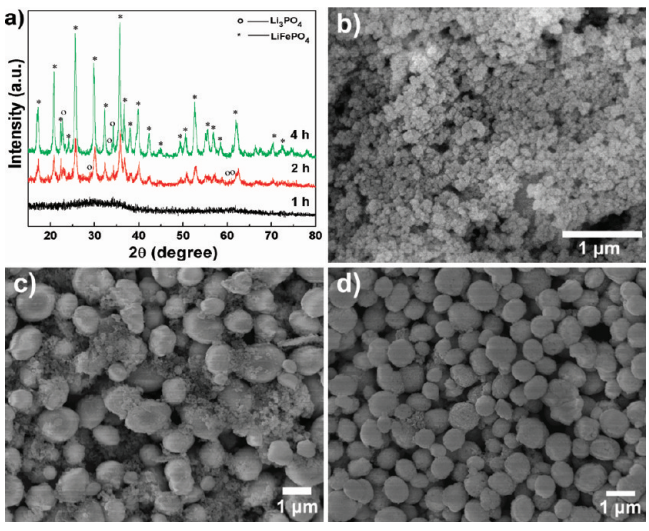


**Figure 5.** (a) XRD patterns and (b,c,d) SEM images of the samples obtained at different reaction times: 1, 2, and 4 h.


dx.doi.org/10.1021/jp212063e | J. Phys. Chem. C 2012, 116, 5019−5024

of the product obtained at 1 h indicates the formation of amorphous phase at the initial stage. With increasing the reaction time to 2 h, the diffraction peaks can be indexed as a mixture of $LiFePO_4$ and $Li_3PO_4$ (JCPDS card No. 25−1030), indicating the gradual formation of crystalline phases. After increasing the reaction time to 4 h, the relative intensities of the XRD peaks for $Li_3PO_4$ become weak, whereas the peaks of $LiFePO_4$ turn to be narrow and strong, demonstrating that the crystallinity is improved. With the $Li_3PO_4$ phase vanished, the single phase of $LiFePO_4$ is obtained until prolonging the reaction time to 6 h (Figure 2a). The products obtained at different reaction stages were also analyzed using SEM to reveal the growth process of self-assembled $LiFePO_4$ nano/microspheres. Obviously, the duration of the reaction has a significant effect on the morphology of the product. Figure 5b shows the formation of nanoparticles at the early stage (within 1 h). As time progresses, the as-formed nanoparticles partly assemble into microspheres (seen after 2 h, Figure 5c). With the reaction further proceeding (after 4 h), nano/microspheres are dominant in the product with few unassembled small nanoparticles (Figure 5d). At the end of the reaction (6 h), uniform nano/microspheres are observed as shown in Figure 3a.

On the basis of the XRD and SEM results, a possible growth mechanism of the $LiFePO_4$ nano/microspheres is proposed as schematically illustrated in Figure 6. First, in the precursor

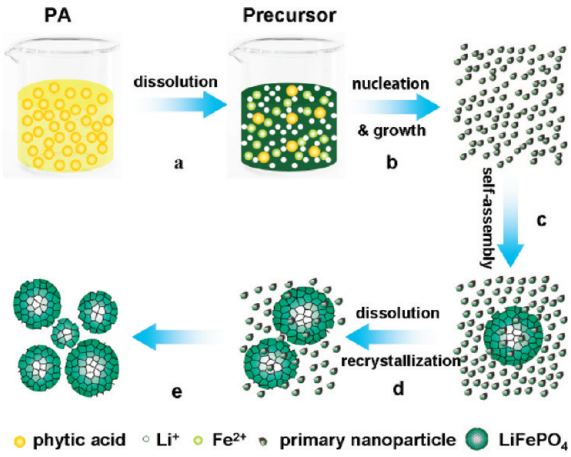


**Figure 6.** Schematic illustration for the self-assembly of $LiFePO_4$ nano/microspheres.

aqueous solution, the organophosphates PA form homogeneous cross-linked complexes with $Fe^{2+}$ (Figure 6, step a).[39] At the initial step of the hydrothermal process, numerous tiny amorphous metal phosphate nuclei form quickly, followed by the growth of the nuclei at the expense of the smaller ones, based on the well-known Ostwald ripening process (Figure 6, step b).[40] In the subsequent process, driven by the minimization of the surface free energy of the system, the small primary nanoparticles begin to assemble together and crystallize to form $Li_3PO_4$ and $LiFePO_4$ (Figure 6, step c). With the temperature and pressure increasing steadily during hydrothermal aging, this intermediate phase dissolves and recrystallizes to form $LiFePO_4$ nuclei due to the large solubility and low stability of $Li_3PO_4$ compared with $LiFePO_4$ in water (Figure 6, step d). When the reaction time reaches 6 h, the $Li_3PO_4$ phase is completely dissolved, and more newly formed $LiFePO_4$ nanoparticles continually assemble into the final microspheres (Figure 6, step e). The formation of $LiFePO_4$ is based on a dissolution−recrystallization process, accompanied by the phase transformation from one material to another material.[27,41] It is believed that the assembly of the nano/microspheres depends on many aspects, for example, PA effect as a phosphorus source and biotemplate, the surface interaction, and the intrinsic character of $LiFePO_4$.

**3.3. Electrochemical Properties.** In order to test the potential application of the $LiFePO_4$/C nano/microspheres as cathode materials for LIBs, the electrochemical performances with respect to Li insertion/extraction were investigated. Figure 7a shows the galvanostatic charge/discharge voltage profiles of the $LiFePO_4$/C nano/microspheres cycled at 0.1 C (completing the discharge or charge process in 10 h). The initial discharge specific capacity is 139 mA h $g^{-1}$, accompanied with capacity increases and gradually levels off at about 155 mA h $g^{-1}$ after 20 cycles. It can also be seen that the polarization between the charge and the discharge plateaus decreases to 50 mV from 120 mV, which is consistent with the gradually increased anodic/cathodic current and the gradually decreased overpotential between the two peak potentials in the initial three CV cycles (Figure S3 in Supporting Information). These phenomena can be mainly ascribed to the progressive penetration of the liquid electrolyte into the particles' interior. Figure 7b,c shows the rate capability and cycling performance of the $LiFePO_4$/C nano/microsphere electrode. The electrode is charged at 0.1 C for each charging step and then discharged at gradually increased rates. At each C-rate, the electrode exhibits flat voltage plateaus (Figure 7b). Even at a 5 C rate (850 mA $g^{-1}$), the discharge voltage plateau is still higher than 3.2 V (vs $Li^+$/Li), and the delivered capacity exceeds 90 mA h $g^{-1}$. The results indicate that the $LiFePO_4$/C nano/microsphere electrode has low polarization, good electrical conductivity, as well as good rate capability. In addition, when the current rate is changed back to 0.1 C after 70 cycles, the electrode is able to retrieve its reversible capacity of 153 mA h $g^{-1}$, showing that the $LiFePO_4$/C nano/microsphere has a good stability after long time cycles at high rates. Another excellent property of the $LiFePO_4$/C nano/microspheres is the superior cycling performance. The reversible discharge capacity remains approximately 120 mA h $g^{-1}$ without obvious capacity fading over 100 cycles at 1 C (Figure 7d).

The results clearly demonstrate that the $LiFePO_4$/C nano/microspheres with high tap density, fine specific capacity, good cycling stability, and high rate capability are promising cathode materials for LIBs. These properties could be attributed to the following factors: (1) the nanosized building blocks of $LiFePO_4$ nanoparticles in the $LiFePO_4$/C microspheres provide shorter diffusion distance for Li ions and hence reduce the time needed for Li ions to migrate into the $LiFePO_4$ lattices. (2) The carbon nanocoating layer on the surface of crystalline $LiFePO_4$ could effectively enhance the electrical conductivity and fasten the transport of electrons,[22] while the nanosized voids between the carbon layers and the $LiFePO_4$ particles could significantly facilitate the diffusion of Li ions from the $LiFePO_4$ lattices into the electrolyte, and vice versa.[18] (3) The robust $LiFePO_4$/C microspheres could greatly decrease the possibility of local destruction of structures induced by large lithium ion flux, especially at high charge/discharge rates. Furthermore, the micrometer-sized assemblies of the $LiFePO_4$/C nano/microspheres lead to the high tap density and hence the improved volumetric energy density compared with tiny nanoparticles. In addition, it also promises ease of process of the cathodes.


dx.doi.org/10.1021/jp212063e | J. Phys. Chem. C 2012, 116, 5019−5024

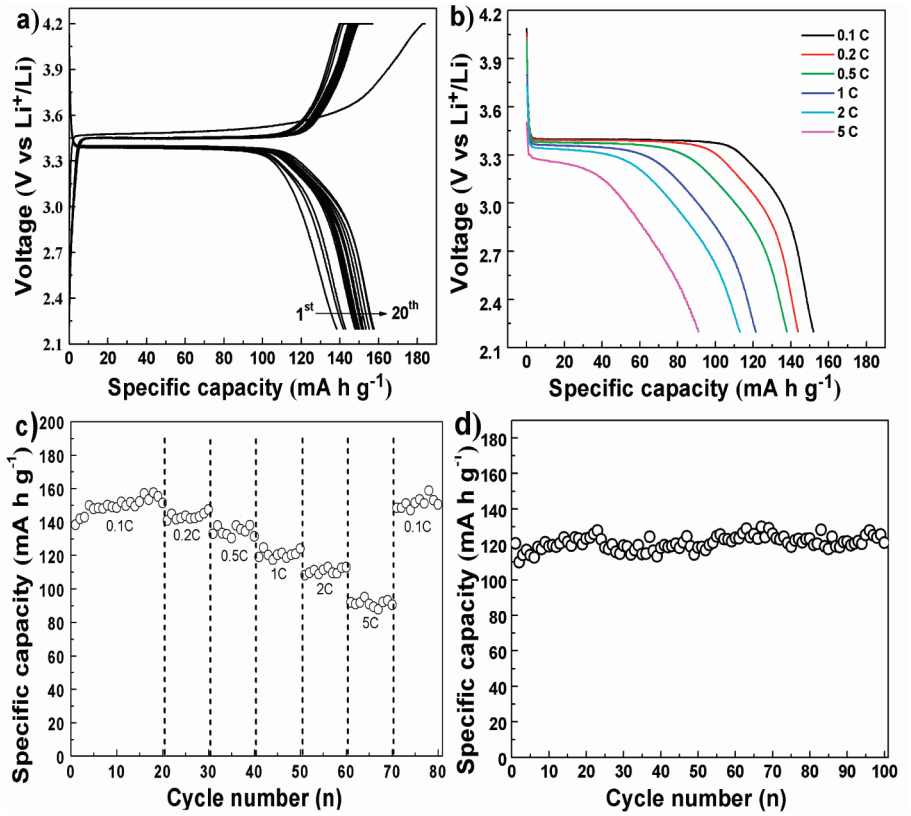


**Figure 7.** Electrochemical characterizations of the $LiFePO_4$/C nano/microspheres in the voltage range of 2.2−4.2 V (vs $Li^+$/Li). (a) Glavanostatic charge/discharge voltage profiles at 0.1 C for the first 20 cycles. (b) Discharge voltage profiles at various discharge rates. (c) Rate performance. (d) Cycling performance at 1 C.

## 4. CONCLUSIONS

A facile hydrothermal method has been developed to synthesize $LiFePO_4$ nano/microspheres employing PA as a novel phosphorus source. The micrometer-sized spheres are self-assembled by nanometer-sized particles of $LiFePO_4$ side by side in an ordered fashion with the help of PA. After carbon coating, the as-obtained $LiFePO_4$/C nano/microspheres exhibit a high tap density of 1.2 g $cm^{-3}$, a high reversible specific capacity of 155 mA h $g^{-1}$ at 0.1 C, as well as excellent rate capability and cycling performance, which make them superior cathode materials for LIBs. The superior properties could be attributed to the nanosized building blocks, the carbon nanocoating layer, the hierarchical structure, and the sphere-like morphology of the product. Our approach for the preparation of $LiFePO_4$ by using PA as the phosphorus source may open new prospects for utilization of biomass to produce high performance cathode materials for LIBs. The assembly strategy is not restricted to the $LiFePO_4$ nano/microspheres, and ongoing work shows that it can be extended to other useful phosphate cathode materials such as $LiMnPO_4$ and the solid solutions of $LiFePO_4$ and $LiMnPO_4$ (i.e., $LiMn_xFe_{1-x}PO_4$, $0 \le x \le 1$).

## ■ ASSOCIATED CONTENT

### Supporting Information

Raman spectra of the $LiFePO_4$/C nano/microspheres. SEM image and corresponding elemental maps of C, Fe, P, and O, and EDS spectrum of the $LiFePO_4$ nano/microspheres before and after carbon coating. CVs of the $LiFePO_4$/C nano/microspheres at a scan rate of 0.1 mV $s^{-1}$. This material is available free of charge via the Internet at http://pubs.acs.org.

## ■ AUTHOR INFORMATION

### Corresponding Author

*E-mail: ygguo@iccas.ac.cn.

### Notes

The authors declare no competing financial interest.

## ■ ACKNOWLEDGMENTS

This work was supported by the National Natural Science Foundation of China (Grant Nos. 91127044 and 21121063), the National Key Project on Basic Research (Grant Nos. 2011CB935700 and 2009CB930400), the WCU program through NRF funded by MEST (R32-2009-000-20074-0), and the Chinese Academy of Sciences.

## ■ REFERENCES

(1) Armand, M.; Tarascon, J. M. *Nature* **2008**, *451*, 652.
(2) Maier, J. *Nat. Mater.* **2005**, *4*, 805.
(3) Li, H.; Wang, Z.; Chen, L.; Huang, X. *Adv. Mater.* **2009**, *21*, 4593.
(4) Padhi, A. K.; Nanjundaswamy, K. S.; Goodenough, J. B. *J. Electrochem. Soc.* **1997**, *144*, 1188.
(5) Chung, S. Y.; Bloking, J. T.; Chiang, Y. M. *Nat. Mater.* **2002**, *1*, 123.
(6) Herle, P. S.; Ellis, B.; Coombs, N.; Nazar, L. F. *Nat. Mater.* **2004**, *3*, 147.
(7) Amin, R.; Balaya, P.; Maier, J. *Electrochem. Solid-State Lett.* **2007**, *10*, A13.
(8) Saravanan, K.; Reddy, M. V.; Balaya, P.; Gong, H.; Chowdari, B. V. R.; Vittal, J. J. *J. Mater. Chem.* **2009**, *19*, 605.
(9) Yamada, A.; Chung, S. C.; Hinokuma, K. *J. Electrochem. Soc.* **2001**, *148*, A224.

(10) Ellis, B.; Kan, W. H.; Makahnouk, W. R. M.; Nazar, L. F. *J. Mater. Chem.* **2007**, *17*, 3248.
(11) Nan, C.; Lu, J.; Chen, C.; Peng, Q.; Li, Y. *J. Mater. Chem.* **2011**, *21*, 9994.
(12) Rangappa, D.; Sone, K.; Ichihara, M.; Kudo, T.; Honma, I. *Chem. Commun.* **2010**, *46*, 7548.
(13) Manthiram, A.; Murugan, A. V.; Sarkar, A.; Muraliganth, T. *Enengy Enviorn. Sci.* **2008**, *1*, 621.
(14) Lim, J.; Mathew, V.; Kim, K.; Moon, J.; Kim, J. *J. Electrochem. Soc.* **2011**, *158*, A736.
(15) Su, J.; Wei, B. Q.; Rong, J. P.; Yin, W. Y.; Ye, Z. X.; Tian, X. Q.; Ren, L.; Cao, M. H.; Hu, C. W. *J. Solid State Chem.* **2011**, *184*, 2909.
(16) Liu, H.; Cao, Q.; Fu, L. J.; Li, C.; Wu, Y. P.; Wu, H. Q. *Electrochem. Commun.* **2006**, *8*, 1553.
(17) Bilecka, I.; Hintennach, A.; Rossell, M. D.; Xie, D.; Novak, P.; Niederberger, M. *J. Mater. Chem.* **2011**, *21*, 5881.
(18) Hu, Y. S.; Guo, Y. G.; Dominko, R.; Gaberscek, M.; Jamnik, J.; Maier, J. *Adv. Mater.* **2007**, *19*, 1963.
(19) Kang, B.; Ceder, G. *Nature* **2009**, *458*, 190.
(20) Wu, X. L.; Jiang, L. Y.; Cao, F. F.; Guo, Y. G.; Wan, L. J. *Adv. Mater.* **2009**, *21*, 2710.
(21) Sun, C.; Rajasekhara, S.; Goodenough, J. B.; Zhou, F. *J. Am. Chem. Soc.* **2011**, *133*, 2132.
(22) Wang, Y.; Hosono, E.; Wang, K.; Zhou, H. *Angew. Chem., Int. Ed.* **2008**, *47*, 7461.
(23) Oh, S. W.; Myung, S. T.; Oh, S. M.; Oh, K. H.; Amine, K.; Scrosati, B.; Sun, Y. K. *Adv. Mater.* **2010**, *20*, 4842.
(24) Cao, A. M.; Hu, J. S.; Liang, H. P.; Wan, L. J. *Angew. Chem.* **2005**, *117*, 4465.
(25) Guo, Y. G.; Hu, J. S.; Wan, L. J. *Adv. Mater.* **2008**, *20*, 2878.
(26) Zheng, S. F.; Hu, J. S.; Zhong, L. S.; Song, W. G.; Wan, L. J.; Guo, Y. G. *Chem. Mater.* **2008**, *20*, 3617.
(27) Yang, H.; Wu, X. L.; Cao, M. H.; Guo, Y. G. *J. Phys. Chem. C* **2009**, *113*, 3345.
(28) Cao, F. F.; Guo, Y. G.; Wan, L. J. *Energy Environ. Sci.* **2011**, *4*, 1634.
(29) Schnepp, Z.; Yang, W.; Antonietti, M.; Giordano, C. *Angew. Chem., Int. Ed.* **2010**, *49*, 6564.
(30) Xia, Y.; Zhang, W.; Huang, H.; Gan, Y.; Xiao, Z.; Qian, L.; Tao, X. *J. Mater. Chem.* **2011**, *21*, 6498.
(31) Sugunan, A.; Melin, P.; Schnürer, J.; Hilborn, J. G.; Dutta, J. *Adv. Mater.* **2007**, *19*, 77.
(32) Wu, X. L.; Chen, L. L.; Xin, S.; Yin, Y. X.; Guo, Y. G.; Kong, Q. S.; Xia, Y. Z. *ChemSusChem* **2010**, *3*, 703.
(33) Wu, X. L.; Wang, W.; Guo, Y. G.; Wan, L. J. *J. Nanosci. Nanotechnol.* **2011**, *11*, 1897.
(34) Cao, L.; Wang, W.; Yang, C.; Yang, Y.; Diana, J.; Yakupitiyage, A.; Luo, Z.; Li, D. *Enzyme Microb. Technol.* **2007**, *40*, 497.
(35) Cassagneau, T.; Fendler, J. H.; Johnson, S. A.; Mallouk, T. E. *Adv. Mater.* **2000**, *12*, 1363.
(36) Arnold, G.; Garche, J.; Hemmer, R.; Strobele, S.; Vogler, C.; Wohlfahrt-Mehrens, M. *J. Power Sources* **2003**, *119*−*121*, 247.
(37) Rho, Y. H.; Nazar, L.F.; Perry, L.; Ryan, D. *J. Electrochem. Soc.* **2007**, *154*, A283.
(38) Burba, C. M.; Frech, R. *J. Electrochem. Soc.* **2004**, *151*, A1032.
(39) Rodrigues-Filho, U. P.; Vaz, S.; Felicissimo, M. P.; Scarpellini, M.; Cardoso, D. R.; Vinhas, R. C. J.; Landers, R.; Schneider, J. F.; McGarvey, B. R.; Andersen, M. L. *J. Inorg. Biochem.* **2005**, *99*, 1973.
(40) Ostwald, W. Z. *Phys.Chem.* **1900**, *34*, 495.
(41) Qin, X.; Wang, X.; Xiang, H.; Xie, J.; Li, J.; Zhou, Y. *J. Phys. Chem. C* **2010**, *114*, 16806.

# Supporting Information for

# Self-Assembled $LiFePO_4$/C Nano/Microspheres by Using Phytic Acid as Phosphorus Source

*Jing Su,[†] Xing-Long Wu,[†] Chun-Peng Yang,[†] Jong-Sook Lee,[‡] Jaekook Kim,[‡] and Yu-Guo Guo*[,†]*

[†] Beijing National Laboratory for Molecular Sciences (BNLMS), Institute of Chemistry, Chinese Academy of Science (CAS), Beijing 100090, P. R. China

[‡] School of Materials Science and Engineering, Chonnam National University (WCU), Gwangju 500-757, Republic of Korea

* To whom correspondence should be addressed. E-mail: ygguo@iccas.ac.cn

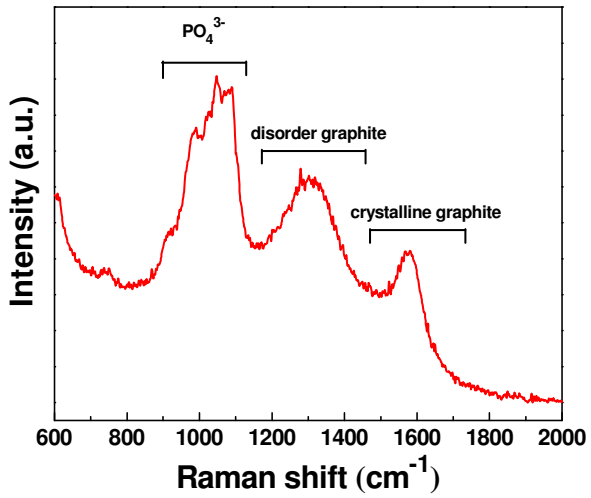


**Figure S1.** Raman spectra of the as-synthesized $LiFePO_4$/C nano/microspheres.

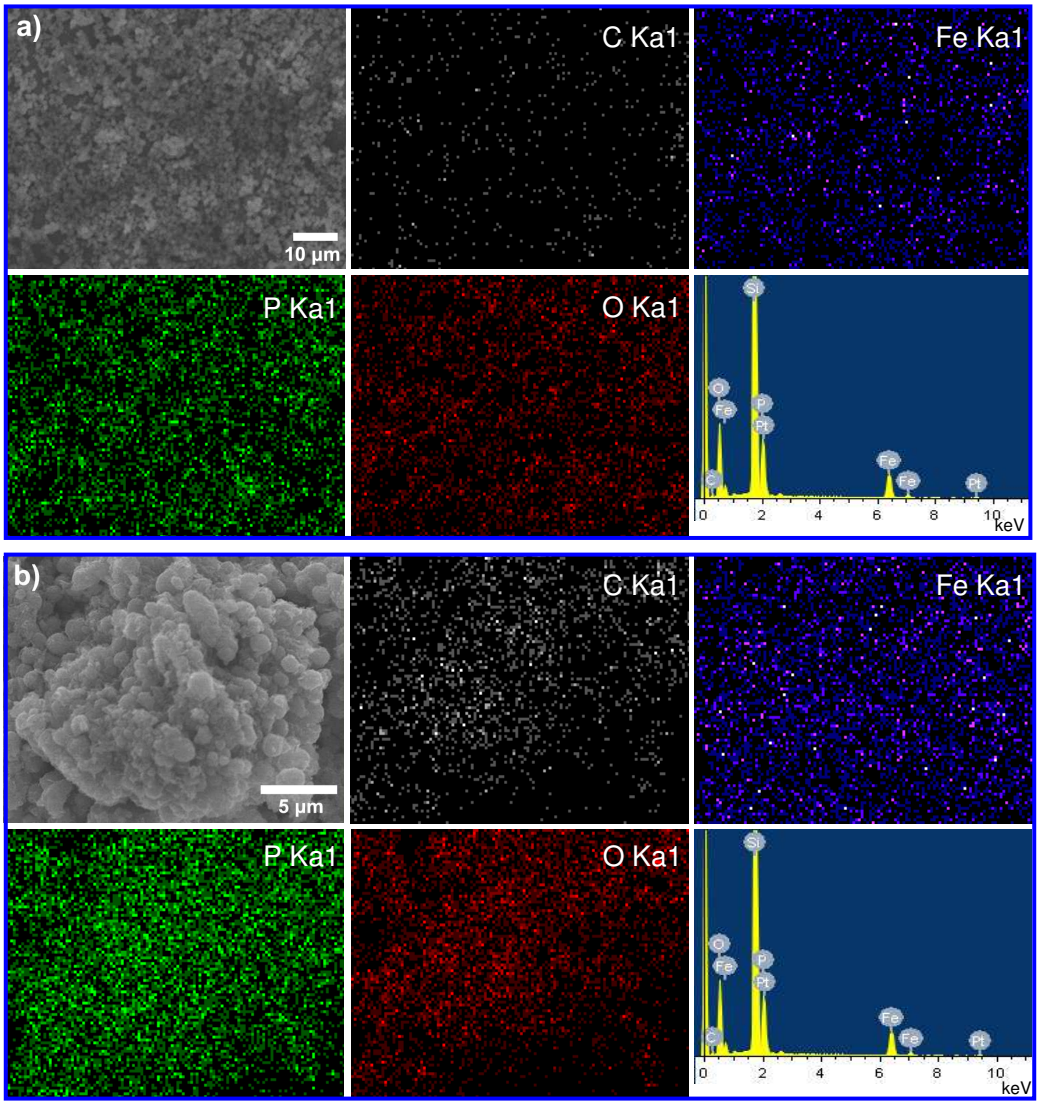


**Figure S2.** SEM image, the corresponding elemental maps of C, Fe, P, O and EDS spectrum of the $LiFePO_4$ nano/microspheres before and after carbon coating. The peaks of Pt and Si originate from sprayed platinum on the surface of test sample and Si substrate, respectively.

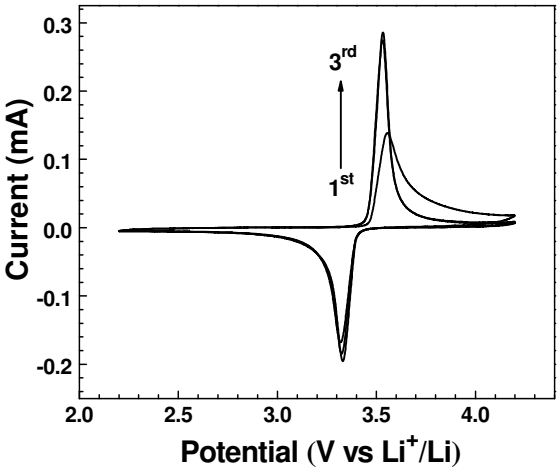


**Figure S3.** CVs of the as-synthesized $LiFePO_4$/C nano/microspheres at a scan rate of 0.1 mV $s^{-1}$.